Journal of Analytical and Applied Pyrolysis 125 (2017) 136–143

Contents lists available at ScienceDirect

Journal of Analytical and Applied Pyrolysis

journal homepage: www.elsevier.com/locate/jaap

Liquefaction of wood and its model components

M. Castellví Barnés[a], M.M. de Visser[a,1], G. van Rossum[b], S.R.A. Kersten[a], J.-P. Lange[a,b,*]

[a] University of Twente, Sustainable Process Technology, P.O. Box 217, Enschede 7500AE, The Netherlands
[b] Shell Global Solutions International B.V., Shell Technology Centre Amsterdam, P.O. Box 38000, Amsterdam 1030BN, The Netherlands

ARTICLE INFO

Keywords:
Liquefaction
Biocrude
Carbohydrate
Lignin
Characterisation

ABSTRACT

Pinewood and various model components were liquefied to bio-oil at 300–310 °C in 1-methylnaphthalene to study the chemistry of the liquefaction process. Cellulose, amylopectin and organosolv lignin were used as model components for the cellulose, hemicellulose and lignin parts of the wood. Furthermore, a few experiments with glucose and wood were performed for a better understanding of the process. The liquefaction products were analysed by ^{13}C NMR, FTIR, Gel Permeation Chromatography (GPC), GC–MS and C:H:O analysis (elemental analysis). The results indicated that the carbohydrates result in char, gas and light biocrude while the lignin leads mainly to light and heavy biocrude. However, the biocrude shows a very similar phenolic character is all cases, even when coming from carbohydrates. Similarities and differences with liquefaction in near/supercritical water or with pyrolysis are highlighted.

1. Introduction

The increase in energy demand, the growing concern for climate change and the need for safe and reliable energy supplies, has stimulated the development of renewable alternatives to the conventional fossil energy sources. One renewable alternative, the biofuels, is particularly attractive for the transport sector because biofuels have a high energy density and are compatible with the existing fuel infrastructures. Lignocellulosic residues from agriculture and forestry are a promising feedstock the production of sustainable biofuels [1–3]. One option to convert lignocellulose to biofuel is their direct liquefaction to biocrude and subsequent processing conventional oil refinery; an approach that has been researched extensively in the 80s [4–7] and has regain of popularity recently [8–10]. Much of this research is using light-boiling solvents such as water, ethanol or acetone and operating at near-critical or super-critical conditions. The high operating pressures and corrosiveness of the medium poses severe challenges at technical scale, e.g. expensive metallurgy and very difficult feeding of the biomass. Our group, therefore, chose to revisit an alternative approach based on the use of cheap high-boiling solvents, more specifically recycled biocrude [11,12], or cheap aromatic refinery streams [13,14], High-pressure hydrogen or syngas was also omitted, in contrast to much of the earlier studies. A similar approach is also being investigated by other groups [15–17].

The switch from low-boiling and nucleophilic solvents, particularly water, to high-boiling and largely apolar solvents is suspected to affect the chemistry of the liquefaction process. Investigating this chemistry is fairly challenging, however, because the organic solvent is masking much of the properties of the biocrude, particularly when the liquefaction results in a heavy biocrude that consists mainly of components that are out of range of common GC and GC/MS analysis. We, therefore, developed a GPC fractionation method to separate the high-boiling solvent from the biocrude and applied FTIR, ^{13}C NMR and element analysis to characterise the biocrude [18]. More recently, we applied this method to revisit the effect of solvent [19].

The present paper is applying the same analytical approach to investigate the chemistry of wood liquefaction. To this end, pinewood and several model components were used as feedstock for liquefaction in 1-methylnapthalene. Cellulose, amylopectin, lignin and glucose were selected as model for wood components while Methylnaphthalene was selected as model for aromatic refinery streams such as vacuum gasoil (VGO) or light cycle oil (LCO), which were found promising liquefaction media [13,14,16,17]. The results are then compared with results obtained in near/super-critical water.

2. Materials and methods

2.1. Materials

Pinewood was purchased from Rettenmaier & Söhne GmbH (Germany), grinded and sieved to a particle size below 0.5 mm and, finally, dried at 105 °C for 24 h. The composition of the wood is shown

* Corresponding author at: University of Twente, Sustainable Process Technology, P.O. Box 217, Enschede 7500AE, The Netherlands.
E-mail address: jean-paul.lange@shell.com (J.-P. Lange).
[1] Present address: Gunvor Group Ltd, The Netherlands.

http://dx.doi.org/10.1016/j.jaap.2017.04.008
Received 16 September 2016; Received in revised form 3 April 2017; Accepted 4 April 2017
Available online 20 April 2017

in Table S1 in supplementary information. Crystalline cellulose (Avicel PH-101, degree of polymerisation of 200) was purchased from Sigma Aldrich and used as model component for the cellulose present in the wood. Maize Amylopectin from Sigma Aldrich was chosen as model component for hemicellulose, which cannot be isolated from the other wood constituents. Organosolv lignin from pinewood was prepared following the method described by Huijgen et al. [20]. D-(+)-Glucose was purchased from Sigma-Aldrich with a purity ≥99.5%.

2.2. Experimental setup and procedure

As detailed elsewhere [21], the liquefaction experiments were performed in a 45 ml autoclave made of Inconel 825 and equipped with a mechanical stirrer and Pico Log recording of pressure and temperature readings. The autoclave was placed in an explosion-proof cell and operated from the outside. A total of 20 or 30 g of biomass and solvents (methylnaphthalene) were introduced in the autoclave, which was then closed tightly and flushed with N_2 for oxygen removal and a leak test. The autoclave was submerged into fluidised sand heated at the reaction temperature and, after liquefaction, immersed in a cold water bath to stop the reactions. The non-condensable gas product was collected once the autoclave was at room temperature. The autoclave was then opened its content was filtered to produce a biocrude and the residual solid. The solid was washed with acetone and dried at 105 °C for 24 h. The acetone wash product was dried and the residual material was added to the biocrude.

2.3. Product definition and calculation

All the yields reported in this paper are expressed in carbon percentage (C%) and based on wood input, and were calculated using the following equations:

$$\text{Gas yield (C\%)} = (\text{mole } C_{gas}*12)/(\text{gram wood}*w\%\ \text{C in wood})*100$$

$$\text{Solid yield (C\%)} = (\text{gram solid}*w\%\ \text{C in solid})/(\text{gram wood}*w\%\ \text{C in wood})*100$$

$$\text{Biocrude yield (C\%)} = 100 - \text{Gas yield} - \text{Solid yield}$$

$$\text{Vacuum residue yield (C\%)} = (\text{biocrude yield}*\text{Vacuum Residue fraction})$$

$$\text{Distillate yield (C\%)} = (\text{biocrude yield}*\text{Distillate content fraction})$$

Here gas refers to all the non-condensable gases, biocrude refers to the acetone soluble components and solid includes the acetone insoluble components. The vacuum residue (VR) and distillate represent here two hypothetical distillation fractions of the biocrude. The VR fraction was defined as having an apparent molecular weight (Mw_{GPC}) higher than 1000 Da while the distillate fractions was defined has having a Mw_{GPC} between 75 and 1000 Da, as defined below.

$$\text{Vacuum residue fraction} = \text{RID Area}_{Mw > 1000\,Da}/\text{RID Area}_{Mw > 75\,Da}$$

$$\text{Distillate fraction} = \text{RID Area}_{75 < Mw < 1000\,Da}/\text{RID Area}_{Mw > 75\,Da}$$

It should be stressed that the biocrude spontaneously separated into a low-viscosity oil phase and a paste-like tar phase that sticks to equipment parts but dissolves in acetone. Tar and oil were analysed separately but then recombined numerically to define the yields of biocrude, distillate and VR discussed above. The paper will generally limit the discussion to the overall biocrude and its hypothetical distillation fraction (distillate and vacuum residue). The discussion of the natural but ill-defined oil and tar phases will be limited to the product characterisation section when we will look for eventual differences in composition and chemical functionalities. Both oil and tar contained a distillate and VR fraction but the tar was richer in VR, as will be discussed below.

The present definition of biocrude yield was chosen for convenience and reliability. It avoids the risk of counting solvent-based products as biocrude, a phenomenon that has been observed with reactive solvent [19]. However, it also has the weakness of counting eventual missing wood-based carbons as 'biocrude'. Defining the biocrude yield on C-basis rather than the more conventional weight-basis allows ones not to be concerned by the formation and fate of water.

Replication of number of liquefaction experiments of wood in 1-methylnaphthalene under various conditions (e.g. at 270 and 300 °C, for 20 and 30 min with 5 and 10% water) showed a reproducibility of 1–2 C% for char and gas yields and 2–3 C% for biocrude yields.

2.4. Product analysis

2.4.1. Preparative GPC fractionation

For the preparative GPC fractionation, the sample was dissolved in THF and filtered through a 0.45 µm syringe filter. A multidraw kit allowed the injection of 1.5 ml of sample into an Agilent Technologies 1200 system composed of a pre-column (PLgel 25 × 25 mm), a column (PLgel 300 × 25 mm with 5 µm, 500A) and a fraction collector. The fractionation was performed at room temperature during 50 min. The THF of obtained fractions was evaporated under vacuum (10–20 mbar) and at 35 °C to obtain the isolated biocrude fractions. Several fractionations of each sample were performed to obtain enough product (at least 0.3 g) for all the analyses.

2.4.2. GPC

The molecular weight distribution of the unreacted lignin and the biocrude was determined with Gel Permeation Chromatography (GPC). Samples were first dissolved in tetrahydrofuran (THF) and then filtered through a 0.45 µm syringe filter. Afterwards, 20 µl of sample were injected to a system from Agilent Technologies 1200 composed of three columns placed in series (7.5 × 300 mm, particle size 3 µm), a refractive index-detector (RID) and a Variable wavelength detector (VWD) operated at 254 nm. The columns were packed with a highly cross-linked polystyrene–divinylbenzene copolymer gel (Varian, PLgelMIXED-bed E). The measurement was performed at 40 °C during 40 min and with 1 ml/min of THF as eluent. To correlate the retention time of the analysed samples with their molecular weight, calibration was done using polystyrene polymers of various molecular weights (162–29,510 Da) as standard.

2.4.3. ^{13}C NMR

To do quantitative ^{13}C NMR, approximately 0.25 g of sample (without liquefaction solvent) and 0.024 g of $Cr(AcAc)_3$ (relaxation agent) were dissolved in 0.7 ml of deuterated DMSO. The measurements were performed at 40 °C with a Bruker 600 MHz-Avance II NMR spectrometer. The DMSO-d6 signal was used as internal reference and the method utilised was inverse gate decoupling with 5 s of relaxation time and 5000 scans. The integration regions were defined according to Ben et al. and Ingram et al. [22,23] and are shown in Table S2 in supplementary information.

The carbon from an acetal functional group is aliphatic and has two ether substituents. For this reason, acetal carbon (84–105 ppm) was combined with the aliphatic alcohols/ethers (54–84 ppm). However, acetals are derivatives of carbonyl groups and, therefore, could also have been combined with the carbonyl/carboxyl carbon (166–210 ppm). Table S5 in supplementary information shows the ^{13}C NMR integration results of the solvent-free liquefaction oils with the acetals combined with the carbonyl/carboxyl groups. Results are very similar to those depicted in Fig. 3, where acetals are combined with aliphatic alcohols and ethers.

2.4.4. FTIR

Qualitative FTIR analyses were done with a Fourier Transform Infrared Spectrophotometer from Bruker equipped with an Attenuated total reflection device (ATR) and a deuterated triglycine sulfate

detector (DTGS). Absorbance was measured in the range 650–4000 cm^{-1} with an spectral resolution of 4 cm^{-1} and 16 scans were performed. Afterwards, the spectra were baseline corrected and normalised.

2.4.5. Element analysis

The carbon, hydrogen and nitrogen content of solid and biocrude products was determined with an Elemental Analyser Inter Science Flash 2000. The oxygen content of the samples was calculated by difference.

2.4.6. GC–MS

The GC-MS analyses were performed with a gas chromatograph equipped with a mass spectrometer (GC 7890A MS 5975C, from Agilent Technologies). First, 5% of sample was dissolved in acetone and filtered through a Whatman filter with a pore diameter of 0.2 μm. After, 1 μL of sample was injected into the injector port set at 250 °C and with a split ratio of 20:1. The chromatography was operated during 106 min in a capillary column (Varian CP9154 60 m) and with a Helium flow of 2 ml/min. The temperature of the oven was set at 45 °C during 4 min, then increased with a rate of 3 °C/min and finally maintained at 280 °C during 20 min.

2.4.7. Gas analysis (Micro-GC)

Gas was analysed and quantified with a Micro-Gas Chromatograph (Variant CP-4900) that was composed of two columns (Molsieve 5A (10 m) and PPQ (10 m)) and used Helium as a carrier gas. H_2, O_2, N_2, CH_4 and CO were analysed in the Molsieve column, and CO_2, C_2H_4, C_2H_6, C_3H_6 and C_3H_8 in the PPQ column.

2.4.8. Scanning electron microscopy

The morphology of chars was studied with Scanning Electron Microscopy, HR-SEM (Analysis Zeiss MERLIN HR-SEM). The system was equipped with a Hot Field Emission Gun and a detector HE-SE2. Measurements were operated with a voltage of 0.85 kV and a prove current of 15–60 pA.

3. Results

A limited study on process parameters (see supplementary information) resulted in the selection of standard liquefaction conditions that are sufficient to deliver a high biocrude yields and low char yields, namely 10 w% wood concentration, 5 wt% of water concentration, initial N_2 pressure of 6 bar and 20 min reaction at 300 °C. Lower water concentration, reaction time or reaction temperature resulted in incomplete wood conversion (i.e. solid residue still showing a dominant carbohydrate fingerprint in FTIR), while higher values of these parameters did not significantly improve the oil yield. Crystalline cellulose (Avicel PH-101), amylopectin, organosolv lignin and glucose were then evaluated as model components for the cellulose, hemicellulose and lignin present in the wood. The amylopectin was selected as representative of the hemicellulose because of its amorphous structure, good accessibility and high reactivity for hydrolysis. The organosolv lignin was selected because it is produced under mild conditions and should, thereby, have undergone minimal degradation. Various reaction times where for the various feedstock in attempt to identify potential difference in reaction sequence.

3.1. Product yields

The product yields obtained after liquefaction of wood, cellulose, amylopectin, glucose and lignin at various reaction times are depicted in Fig. 1. All feedstock showed a nearly constant biocrude yield after the initial 20 min of liquefaction (Fig. 1a – N.B.: the apparent slow decrease in biocrude yield observed for cellulose needs experiments at even longer reaction times to be confirmed). The final biocrude yield decreased in the order of lignin > cellulose = wood > amylopectin > glucose. Variations in final biocrude yields is mainly related to opposite variations in solid yield and to a much lesser extend to variations in gas yields, which remains fairly low for all feedstocks (see Fig. 1c–e).

Upon closer inspection, all carbohydrates led to a biocrude that is fairly light (100–1000 Da) and shows a similar Mw distribution, despites large differences in degree of polymerisation of the feedstock (Fig. 1f). Variations in biocrude yields for the carbohydrates is, therefore, dominated by variation in distillate yields (Fig. 1b) more than in Vacuum residue (VR) yield (Fig. 1d). This suggests that the biocrude is formed via a combination of depolymerisation and repolymerisation of carbohydrates or their derivatives. The vacuum residue seems chemically stable since its yields remain low (< 8 C%) over time. This contrast with the distillate that appears to partly crack to gas at increased reaction time (Fig. 1b and e).

In the case of lignin, the biocrude is reported to be 100 C% at zero reaction time because lignin was found to be soluble in 1-methylnaphthalene above 70 °C, during a blank experiment. Upon conversion, the amount of biocrude barely decreased, with gas and solid being produced in marginal amounts (Fig. 1a, c and e). Lignin conversion mainly consisted of a partial shift from VR to Distillates, i.e. from 80 to 30 C% VR yield and from 30 to 65 C% distillate yield (Fig. 1b and d). During the process, the heaviest components shifted from ~10 kDa up to 30 kDa after 20 min of reaction (Fig. 1f) and then back to ~10 kDa upon extended reaction (see supplementary information). It should be stressed that the lignin biocrude contains more and heavier VR than observed for carbohydrates.

Coming back to the solid product, the solid yield increased in the reverse order of the biocrude yields, namely: lignin > wood ~ cellulose > amylopectin > glucose (Fig. 1c). The more reactive carbohydrate (glucose) led to the highest solid yield, while the most recalcitrant one (cellulose) gave the lowest. The solid residue generally showed an FTIR finger print that betrays an aromatic char-like structure (discussed later). As exception, the solid obtained at the early stage of cellulose liquefaction (after 10 and 15 minutes) still showed a dominant carbohydrate finger print in FTIR, suggesting unconverted cellulose.

The gas yields followed similar trends for the three carbohydrates, with yield increasing rapidly to ~5 C% in the initial stage and more slowly to ~10 C% thereafter (Fig. 1e). The late evolution of gas likely comes from the biocrude, which showed a slight decrease with time. In contrast, lignin produced a very low gas yield (< 2 C%), even after 16 h (960 min) of reaction time.

The high char yields observed for the reactive carbohydrate glucose and amylopectine may have been due to the temporary release of sugars in high concentration. Hence, we performed liquefaction experiments with two different glucose concentrations. Results confirmed that a higher glucose concentration leads to higher char formation (Fig. 2).

In summary, carbohydrates lead to significant char and gas yields and a distillate-rich biocrude (Mw_{GPC} of 75–1000 Da). This contrasts with lignin, which largely dissolves in methylnaphthalene and slowly sees its large fraction of VR (Mw_{GPC} > 1000 Da) partly converted to distillate with marginal formation of char and gas. Among the carbohydrates, the recalcitrant cellulose gives the highest biocrude yield, while the reactive amylopectin and glucose lead to considerably lower oil yields and higher char yields. The behaviour of wood seems to be dominated by its main constituent, the cellulose, with the exception of the production of VR that stems from its lignin content.

3.2. Product characterisation

3.2.1. Biocrude

The biocrude products of lignin, cellulose and amylopectin liquefaction were characterised more in depth. Since the biocrude spontaneously split into an oil and a tar fraction, it seemed convenient to analyse them as such in search for eventual differences in composition

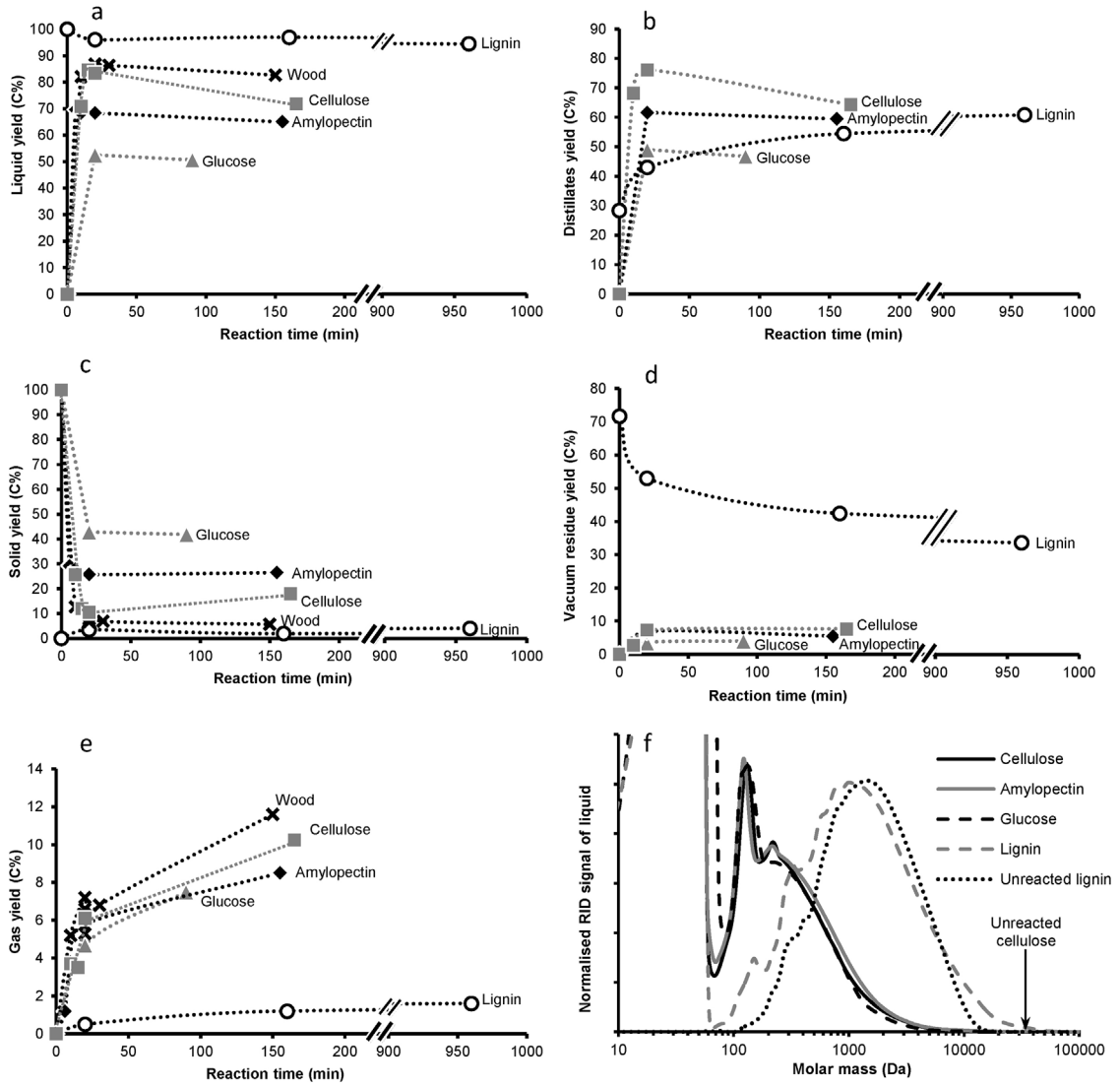

Fig. 1. Product yields of the liquefaction experiments (a–e) and molecular weight distribution of the biocrude for the four model components, unreacted lignin and unreacted cellulose (The Mw of the unreacted cellulose was calculated by multiplying the degree of polymerisation of Avicel pH-101 reported by Rojas et al. and the Mw of a cellulose monomer [24].) (f). Liquefaction experiments of graphs a–e were performed at 300–310 °C with 10 wt% of biomass, 5 wt% of water, and 85 wt% of 1-methylnaphthalene at several reaction times. Liquefaction experiments for graph f were performed for 20 min.

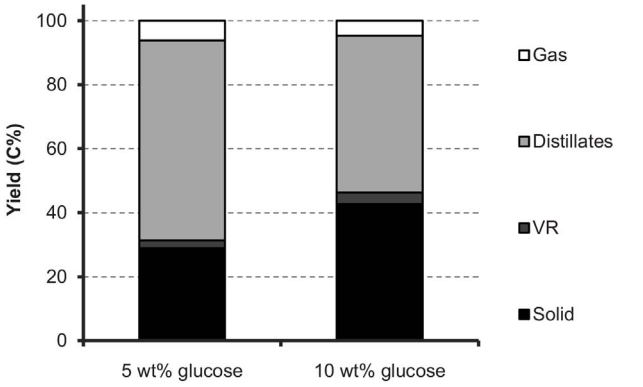

Fig. 2. Product yields from glucose experiments. Liquefaction experiments were performed at 300–310 °C during 20 min, and with 5 wt% of water, 5/10 wt% of glucose and 85/90 wt% of 1-methylnaphthalene.

and chemical functionalities. Hence, the following section will focus on the natural oil and tar fractions rather than the more theoretical distillate and vacuum residue fractions used until now.

Both oil and tar fractions contained methylnaphthalene, distillate and vacuum residue. However, the tar fraction was still richer in heavy components than the oil. The carbohydrate and lignin tars contained components up to 5 and 10 kDa, respectively, whereas both carbohydrate and lignin oils stopped around 2 kDa (see Figs. S4 and S5 in supplementary information). However, their high concentration of 1-methylnaphthalene prevents their characterisation. Methylnaphthalene was, therefore, removed by preparative GPC fractionation, as described in an earlier paper [18]. This may have led to the removal of some light biocrude molecules as well, however. These were investigated by means of GC–MS analysis of the non-fractionated oils. All other analysis, FTIR, EA and ^{13}C NMR, were carried out on the solvent-free oil and tar after preparative GPC fractionation. The solid and gas products were characterised by FTIR + EA and GC, respectively.

Qualitative GC-MS analysis of the oils (prior to removal of methylnaphthalene) revealed a series of aromatic components, mainly 1-methylnaphthalene derivatives and nitrogen-containing aromatics that came as impurities with the solvent (see Table 6 and Fig. 20, in Supplementary Information). Besides that, the carbohydrate oils also presented light furanic and phenolic components in significant concentrations, as well as some cyclopentenones. Smaller but significant

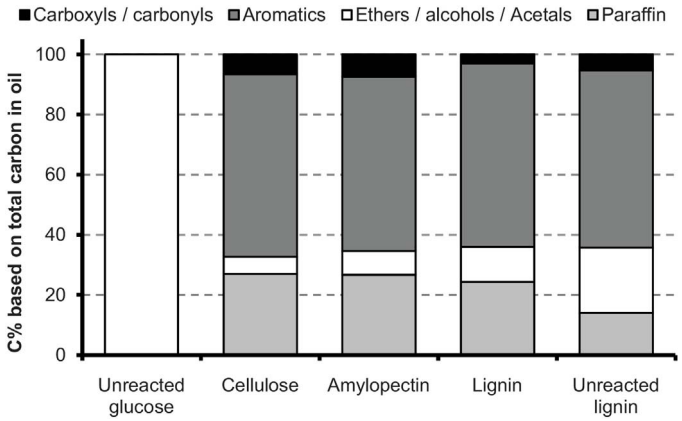

Fig. 3. ^{13}C NMR integration results of unreacted lignin and solvent-free liquefaction oils. (^{13}C NMR assignment reported in supplementary information). Liquefaction experiments were performed at 300–310 °C with a 10 wt% of biomass, a 5 wt% of water, an 85 wt% of 1-methylnaphthalene during 20 min.

concentrations of small oxygenated molecules, such as acetic acid or hexane-2,5-dione were also observed. The lignin oil contained significant amount of phenolic components with unsaturated alkyl chains, methoxy, aldehyde or ketone groups. The unmistakable presence of phenolic products was expected in the lignin oil but noteworthy for carbohydrate oils. This point will be addressed later in the discussion part of this paper.

^{13}C NMR analysis of the oils (Fig. 3) revealed very similar chemical functionality for the carbohydrate and lignin oils: e.g. approximately 60% of the carbons are aromatic-like (105–166 ppm) and ~25% are paraffinic-like (1–54 ppm). It should however be stressed that the aromatic-like components are meant in the wide sense of the term, i.e. they include furanic and phenolic components which cannot be differentiated by means of ^{13}C NMR. In fact, all oils resemble unreacted lignin and just differ in the higher content of paraffin-like components (24–27 C% vs. 14 C% at 1–54 ppm) and a lower concentration of aliphatic alcohols/ethers (6–12 C% vs. 22 C% at 55–105 ppm). Thus, carbohydrates, which are mainly composed of aliphatic alcohol carbons, were converted to a lignin-like product with high aromatic and significant paraffinic carbon content.

The lower content of aliphatic ether/alcohol and higher content paraffinic-like components in the lignin oil (vs. unreacted lignin), suggests that the lignin decomposes through the cleavage of ether bonds and the simultaneous formation of aliphatic species. Lignin presents two major types of ether: primary ethers from the methoxy substituents, and secondary ethers that connect the aromatic units composing the lignin. According to ^{13}C NMR results, both primary and secondary ethers are broken during lignin liquefaction (see Supplementary Information).

Elemental analyses confirmed the similarity of all the oils with unreacted lignin. The Van Krevelen diagram in Fig. 4 indicates a modest decarboxylation/decarbonylation of these biocrudes, which agrees with the increase in gas yield and the decrease in biocrude yield observed, especially, for the carbohydrates (Fig. 1). The oils present slightly higher effective H/C ratio than the corresponding solid residue (see Supplementary Information). These observations are well in line with those made for the liquefaction oil of wood reported earlier [18].

Although cellulose, amylopectin and lignin led to very similar char and oil products, larger differences were observed between their tars. When comparing the oils and tars from cellulose and amylopectin, NMR revealed that tars have a higher content of unconverted or partially unconverted carbohydrates than the oils. This was observed through the higher concentration of oxygenated groups (alcohols, ethers, carbonyls and carboxyls; see Supplementary Information) in the tar. Accordingly, elemental analysis showed higher oxygen content in the tar than in the lighter oil (Fig. 4), and FTIR spectra (see Figs. S4 and S6 in Supplementary Information) of bio-tars presented larger sugar C–O

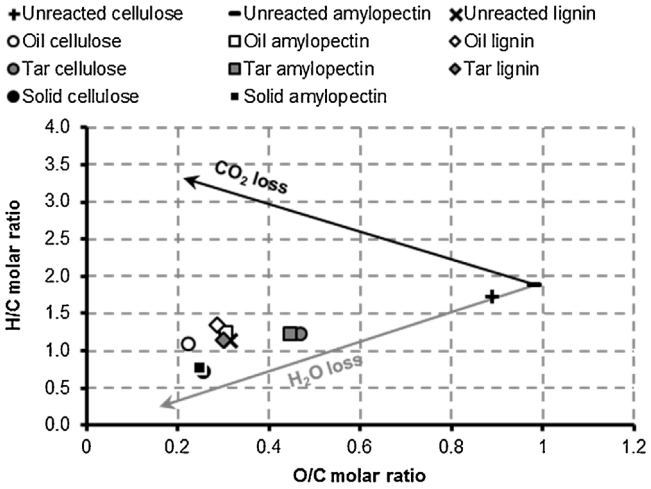

Fig. 4. Van Krevelen diagram of model components and the solid and biocrude obtained after their liquefaction. Liquefaction experiments were performed at 300–310 °C with a 10 wt% of biomass, a 5 wt% of water, an 85 wt% of 1-methylnaphthalene during a reaction time of 20 min.

stretching band (1000 cm^{-1}) and carbonyl/carboxyl band (1710 cm^{-1}) than the spectra of oils.

In contrast, the lignin tar showed the same NMR and elemental composition than unreacted lignin, while the lignin oil presented significantly more paraffin-like components and less alcohol/ether groups (see Fig. 4 and Table S5 and Fig. S2 in Supplementary Information). The GPC chromatograms also revealed marginal differences in Mw distribution between tar and unreacted lignin, with the exception of a heavier tail that stretched to 30 kDa instead of 10 kDa for unreacted lignin (see Fig. S4, Supplementary Information). In contrast, the oil was much lighter with its highest Mw around 3 kDa only. The presence of a heavy tail in tar suggests the presence of polymerisation reactions during liquefaction.

3.2.2. Solid

FTIR spectroscopy and elemental analysis revealed an aromatic char-like structure for nearly all the solid residues. With sufficiently long reaction times, all the feedstock led to the formation of an aromatic solid (char) that had a low hydrogen and oxygen content (C:H:O = 1:0.75:0.25) and showed an FTIR spectrum with broad and undefined bands, as reported earlier for wood-derived char [18]. The only exceptions encountered were the solids obtained at the initial stages of cellulose and lignin liquefactions. For reaction times below 20 min, cellulose solid consisted mainly of unconverted cellulose and presented the typical carbohydrate FTIR bands (e.g. C–O stretching

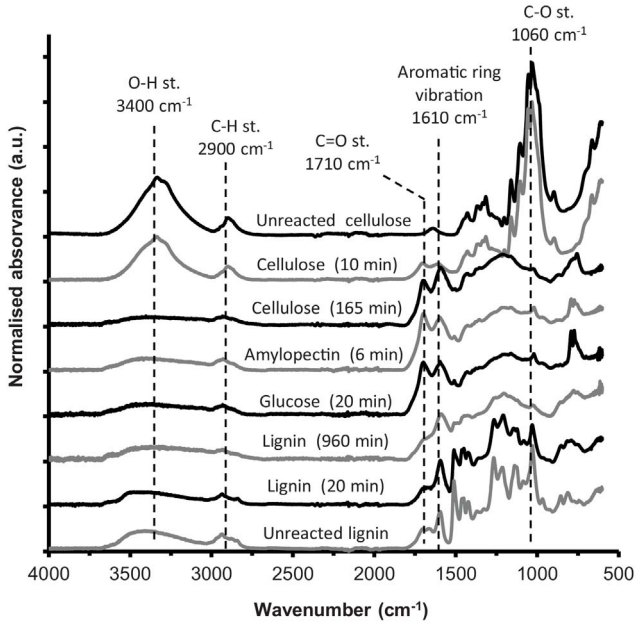

Fig. 5. FTIR spectra of model components and solid residues. Liquefaction experiments were performed at 300–310 °C with a 10 wt% of biomass, a 5 wt% of water, an 85 wt% of 1-methylnaphthalene at the specified reaction times.

band at 1000 cm^{-1}, Fig. 5). Likewise, the solid residue from lignin liquefaction at short reaction times presented an FTIR spectrum very similar to that of the unreacted lignin (Fig. 5). Upon extended reaction time, however, the lignin solid lost some chemical functionality, as reflected in the loss of definition of the FTIR spectra and the decrease of the bands typically attributed to oxygenated functional groups, namely the O–H stretching band from the phenol groups (3400 cm^{-1}), the C=O stretching band typical of carbonyl and carboxyl groups (1710 cm^{-1}), the broad band at 1200 cm^{-1} attributed to aromatic oxygenates [18,21] and the C–O stretching band corresponding to aliphatic ether or alcohol groups (1000 cm^{-1}).

The Van Krevelen diagram depicted in Fig. 4 confirms that the solid residues from cellulose and amylopectin have the same composition after 20 min of liquefaction. The two solids have similar oxygen content than lignin, but they are leaner in hydrogen.

Despite their similar chemical composition, SEM analysis showed completely different morphologies for cellulose and amylopectin solids. While cellulose solid presented a fibrous structure (Fig. S8 in Supplementary Information), amylopectin solid consisted on large glass-like particles with entrapped gas bubbles (see Fig. S9, Supplementary Information). Few spheres were observed in the surface of the amylopectin solid particles. After 20 min if liquefaction, glucose produced a solid similar to the amylopectin solid, but with a rougher surface, and smaller entrapped gas bubbles (see Fig. S10, Supplementary Information). The shattering of the amylopectin and glucose solid particles illustrated in Supplementary Information was caused by the grinding performed during sample preparation for FTIR analysis.

3.2.3. Gas

For all liquefaction experiments, 70–80 vol% of CO_2 and 20–25 vol % of CO were found in the gas. Methane was only formed in marginal amounts. For the carbohydrates, the gas composition did not change with increasing reaction time, but for lignin, a slight increase in CH_4 and H_2 concentration was observed with increasing time.

3.2.4. Summary of characterisation

Summarising the products characterisation, all liquefaction oils resemble unreacted lignin in terms of elemental composition and functional groups. The major differences were found in the compositions and Mw distribution of the tars, which contained unconverted or partially unconverted feedstock. Furthermore, considerably heavier molecules were observed in the lignin biocrude than in the carbohydrates biocrudes. Under complete conversion, all sugars produced an aromatic char-like solid. This char still shows fibrous structure in the case of cellulose but glassy structure is the case of amylopectin and glucose.

4. Discussion

4.1. Origin of aromatic biocrude

The biocrude of carbohydrates and lignin showed similarities in elemental composition (EA) and chemical functionality (NMR and FTIR) but differed mainly in Mw distribution. All biocrudes showed a C:H:O atomic ratio around 1:1.2:0.3 (Fig. 4) and consisted mainly of aromatic-like species (incl. phenolic and furanic species) and to a lesser extend also some paraffinic-like species (i.e. ~60 and ~25 C%, respectively – Fig. 3). However, the Mw distribution differed, being around 100–1000 Da for the carbohydrate biocrude and 300–10,000 Da for the lignin biocrude. The biocrude also differed on another, minor though intriguing points: The light fraction of the biocrude comprised both phenolic and furanic components in the case of carbohydrate but only phenolic components in the case of lignin. We can speculate that this difference is also present in the heavier fractions of the biocrude, but such discrimination could not be made by the present NMR and FTIR analysis and may require more sophisticated analyses such as solid-state 2DPASS ^{13}C NMR spectra or pyrolysis GC–MS [25].

The conversion of carbohydrate to furanics and of lignin to phenolics was expected as it is widely reported in literature [22,26–32]. However, the conversion of carbohydrates to phenolic species is much less documented [5,10]. Several reactions that could lead to phenolic components have been proposed, e.g. the hydration of a furanic ring followed by ring-closure through intramolecular aldol or by electrocyclic reactions and, finally, dehydration [33], aldol condensation of small oxygenates followed by ring-closure and dehydration [34] or Diels–Alder condensation of furans followed by dehydration [35]. Further study is required to confirm the formation of heavy phenolic components during carbohydrate liquefaction and determine the reactions involved.

The chemistry reported here seems to resemble that reported in near/super-critical water. At short residence time (10 s at 320 °C to 0.1 s at 400 °C), cellulose is shown to hydrolyse to oligosugars and decompose to C3–C6 sugars, hydroxyl/keto-aldehydes and furanics [36]. No phenolics are reported under these conditions that minimise consecutive reactions. When processed at longer residence time (15 min at 400 °C in the presence of K_2CO_3), however, glucose, lignin and wood are all converted to a similar biocrude that mainly consists of furanics, cyclopenta(e)nones and phenolic components [37]. Such biocrude is reported to be moderately light for carbohydrates and lignin, with 80% boiling below 540 °C and, thereby, is likely to have a Mw below 600 Da. Such Mw distribution resembles that reported here for carbohydrate. However, it is clearly lighter than observed here for lignin. Hence, the chemistry of lignin liquefaction seems to vary with liquefaction solvent.

4.2. Origin of char and gas

According to the results presented above, char resembles a 'primary' product with mostly carbohydrate origin. Thus, char is not significantly formed from the biocrude product, but from early reaction intermediates such as depolymerised sugars or their derivatives. Even though the chars from cellulose, amylopectin and glucose have a very similar chemical composition (EA and FTIR), they present different morphologies – fibres in the case of cellulose and glassy particles in the case of amylopectin and glucose – which suggest different formation mechan-

isms. The fibrous char produced in low yield from cellulose seem to have resulted from the dehydration and cross-linking on poorly depolymerised cellulose. The glassy particles that are produced at high yields from reactive sugars (glucose and amylopectin) may rather have resulted from the condensation/cross-linking of derivatives of monomeric or highly depolymerised carbohydrates that become poorly soluble beyond a given Mw and, eventually, agglomerate and solidify to glassy char. The higher the concentration of reactive sugars, the higher the probability of condensation to char, as observed in Section 2.3. Interestingly, the char morphologies observed here deviate from those obtained upon acid-hydrolysis of carbohydrates and/or their derivatives [25,38–42]. These humins consisted indeed of aggregates of globular particles, which were presumably formed by desolubilisation of biocrude components into micelles and subsequent condensation within the micelles.

Gas behaves both as a 'primary' and a 'secondary' product and consist mainly of CO_2 and some CO that are liberated from carbohydrates and their derivatives. Lignin liquefaction gives considerably less gas than the sugars.

The char yields reported here seem to deviate to those reported for hydrothermal liquefaction. Indeed, in near/super-critical water, the yields to char is reported to be marginal (< 10%) for cellulose and glucose [10,36,37] but high (~50%) for lignin [10,37]. Differences in char yields are also found with wood as feedstock: under very similar conditions wood is reported to deliver ~25 C% of char in subcritical water [7] vs. the ~5 C% reported in Fig. 1c. Hence, the chemistry unravelled for hydrothermal liquefaction may not fully apply for the liquefaction in aromatic solvent, particularly for the lignin.

4.3. Reaction scheme

The various product fractions show the kinetic behaviour of 'apparent' primary reaction products, as observed and discussed extensively earlier [21]. Indeed, all products are formed at the very early stage of the reaction, without clear induction period. They are subjected to only moderate 'secondary' degradation or formation at long reaction time and deep conversions. The qualification of 'apparent' primary product is use here to indicate that the char, biocrude, and gas may well come from 'true' primary products that are formed at the onset of the reaction but could not be identified, even after resident time as short as 100 s [21]. However, mono- and oligosaccharides have been observed at even shorter residence time of 10 s during liquefaction in near/supercritical water [36]. Such a description is further oversimplified since a few minor deviations from 'apparent' primary kinetic behaviour are observed. Firstly, the cellulose biocrude seems to undergo minor decomposition with time; a point that would need further confirmation. Secondly, the gaseous product shows a slow secondary formation with carbohydrate feedstock that follows the faster primary formation during the initial ~20 min of reaction. Thirdly, a part of the VR is cracked to distillate in the case of lignin.

During the initial stages of the liquefaction, all carbohydrates appear to undergo a series of reversible polymerisation and depolymerisation reactions that are followed by irreversible decomposition (e.g. dehydration) to biocrude. The heavier VR-type intermediates, being not highly soluble in the medium during reaction, deposit on reactor wall and stirrer and, eventually, condense and degrade into glassy char. However, a small fraction the cellulose does not depolymerise at sufficient rate but rather undergo dehydration and condensation reactions, leading to the formation of fibrous char. Meanwhile, lignin is converted to biocrude through cracking reaction and, to a limited extent, also some condensation reactions. The limited condensation reactions temporarily lead to components with increased Mw. However, they are readily overtaken by consecutive cracking reactions to lighter products.

More detailed reaction schemes have been proposed for liquefaction of carbohydrates in near/super-critical conditions [10,37]. These schemes seem applicable to the liquefaction of carbohydrates in aromatic solvent, which lead to a similar biocrude in both media. However, the liquefaction of lignin seems to proceed differently in aromatic solvent than in near/super-critical water. The former leads to heavy biocrude and no char whereas the latter leads to light biocrude and much char. One can therefore expect lignocellulose to behave differently in aromatic solvent than in near/super-critical water. In fact, the nature of solvent has been found to strongly affect the char yield [12,19]. Low char yields seem to require solvents with good affinity with the cellulose, e.g. as expressed in Hildebrand parameter or in Hansen distance [19]. This was tentatively explained by proposing the need for an efficient dissolution of early reaction intermediates, e.g. oligosaccharides or some derivatives, to facilitate their removal from the wood surface and, thereby, depress charing reactions.

4.4. Comparison of liquefaction and fast pyrolysis

Lignin appears to be the most recalcitrant wood component for both liquefaction and pyrolysis processes. However, they lead to different product: lignin liquefaction leads to high vacuum residue yields while its pyrolysis leads to high char yields [43,44]. This observation leads us to formulate the following hypothesis. In pyrolysis, the heavy species are indeed too heavy to evaporate and exit the reactor. Hence, they likely concentrate as liquid film on solid particles and, eventually, overcook to form char [43,44]. During liquefaction, however, these heavies could readily be dispersed and stabilised by the liquefaction solvent and would, therefore, be found as heavy tail in the biocrude [45]. This hypothesis is further supported by the observation of char yields near 80 C% when the 'liquefaction' is run at 300 °C with N_2 of medium [12]. However, we cannot fully discard the role of reaction temperature to explain the difference in behaviour of carbohydrate and lignin during pyrolysis and liquefaction. Running the liquefaction in guaiacol to higher temperature was indeed reported to result a lighter biocrude and more char [21].

The fate of the carbohydrates seems also to vary for liquefaction and pyrolysis. Upon liquefaction, carbohydrates can be converted to char, particularly when present in reactive depolymerised form and at high concentration. Char results from direct condensation of reaction intermediates or dehydration of the initial solid. The fraction of carbohydrates that does not end up in char is converted into light phenolic biocrude. This contrasts also with flash pyrolysis that is capable of cracking all the carbohydrates in volatile anhydrosugars under ideal conditions, e.g. in absence mass transfer limitations [46–48].

5. Conclusions

The results lead to the following conclusions:

- The char is mainly formed from carbohydrates, mainly through precipitation and dehydration of heavy carbohydrate derivatives and, only to a small extent, through dehydration of non-depolymerised cellulose. Char is not formed from lignin and the lignin-like biocrude to any significant extent.
- Similarly, the gas is mainly formed from the carbohydrates and, to a lesser extent, from decomposition of the distillate formed from carbohydrates.
- The biocrude comes from carbohydrates and lignin. The carbohydrates lead mainly to distillate-range products while the lignin leads to both distillates and VR.
- Despite their structural and compositional differences, cellulose, amylopectin and lignin yield all very similar lignin-like biocrudes that are rich in aromatic carbons (~60 C% measured by ^{13}C NMR, which covers both furanic and phenolic species). All biocrudes also contain a significant fraction of paraffinic carbon (~25 C%) and moderate fractions of aliphatic alcohol/ether and carbonyl/carboxyl carbons (~15 C%). Carbohydrates are clearly converted to phenolic

components besides the more expected furanic derivatives.
- The liquefaction of carbohydrates in near/super-critical water shows much similarities to the liquefaction in aromatic solvent that is reported here. However, this does not apply to the liquefaction of lignin, which leads to lighter biocrude and more char than observed here.

Acknowledgements

The authors would like to thank Shell Global Solutions International B.V. for funding this research, and Benno Knaken, Erna Fränzel-Luiten and Bianca Snellink-Ruël for the technical support.

Appendix A. Supplementary data

Supplementary material related to this article can be found, in the online version, at http://dx.doi.org/10.1016/j.jaap.2017.04.008.

References

[1] J. Fargione, J. Hill, D. Tilman, S. Polasky, P. Hawthorne, Science 319 (2008) 1235.
[2] T. Searchinger, R. Heimlich, R.A. Houghton, F. Dong, A. Elobeid, J. Fabiosa, S. Tokgoz, D. Hayes, T.-H. Yu, Science 319 (2008) 1238.
[3] J.-P. Lange, Catalysis for Renewables, Wiley-VCH Verlag GmbH & Co. KGaA, 2007, p. 21.
[4] J.M. Bouvier, M. Gelus, S. Maugendre, Appl. Energy 30 (1988) 85.
[5] O. Theander, Fundamentals of Thermochemical Biomass Conversion, in: R.P. Overend, T.A. Milne, L.K. Mudge (Eds.), Springer Netherlands, Dordrecht, 1985, p. 35.
[6] D.C. Elliott, D. Beckman, A.V. Bridgwater, J.P. Diebold, S.B. Gevert, Y. Solantausta, Energy Fuels 5 (1991) 399.
[7] J.M. Moffatt, R.P. Overend, Biomass 7 (1985) 99–123.
[8] H.-j. Huang, X.-z. Yuan, Prog. Energy Combust. Sci. 49 (2015) 59.
[9] M.K. Jindal, M.K. Jha, Rev. Chem. Eng. 32 (2016) 459.
[10] S.S. Toor, L. Rosendahl, A. Rudolf, Energy 36 (2011) 2328.
[11] S. Kumar, J.P. Lange, G.V. Rossum, S.R.A. Kersten, ACS Sustain. Chem. Eng. 3 (2015) 2271.
[12] G. van Rossum, W. Zhao, M. Castellvi Barnes, J.-P. Lange, S.R.A. Kersten, ChemSusChem (2013) 253.
[13] S. Kumar, A. Segins, J.P. Lange, G. Van Rossum, S.R.A. Kersten, ACS Sustain. Chem. Eng. 4 (2016) 3087.
[14] S. Kumar, J.-P. Lange, G. Van Rossum, S.R.A. Kersten, ChemSusChem 8 (2015) 4086.
[15] S.H. Lee, T. Ohkita, Wood Sci. Technol. 37 (2003) 29.
[16] N. Schwaiger, D.C. Elliott, J. Ritzberger, H. Wang, P. Pucher, M. Siebenhofer, Green Chem. 17 (2015) 2487.
[17] N. Schwaiger, R. Feiner, K. Zahel, A. Pieber, V. Witek, P. Pucher, E. Ahn, P. Wilhelm, B. Chernev, H. Schröttner, M. Siebenhofer, BioEnergy Res. 4 (2011) 294.
[18] M. Castellví Barnés, J.P. Lange, G. van Rossum, S.R.A. Kersten, J. Anal. Appl. Pyrolysis 113 (2015) 444.
[19] M. Castellví Barnés, J. Oltvoort, S.R.A. Kersten, J.-P. Lange, Ind. Eng. Chem. Res. (2017), http://dx.doi.org/10.1021/acs.iecr.6b04086.
[20] W.J.J. Huijgen, A.T. Smit, P.J. de Wild, H. den Uil, Bioresour. Technol. 114 (2012) 389.
[21] S. Kumar, J.-P. Lange, G. Van Rossum, S.R.A. Kersten, Ind. Eng. Chem. Res. 53 (2014) 11668.
[22] H. Ben, A.J. Ragauskas, Energy Fuels 25 (2011) 2322.
[23] L. Ingram, D. Mohan, M. Bricka, P. Steele, D. Strobel, D. Crocker, B. Mitchell, J. Mohammad, K. Cantrell, C.U. Pittman, Energy Fuels 22 (2007) 614.
[24] J. Rojas, A. Lopez, S. Guisao, C. Ortiz, J. Adv. Pharm. Technol. Res. 2 (2011) 144.
[25] I. van Zandvoort, Y. Wang, C.B. Rasrendra, E.R.H. van Eck, P.C.A. Bruijnincx, H.J. Heeres, B.M. Weckhuysen, ChemSusChem 6 (2013) 1745.
[26] M.S. Mettler, S.H. Mushrif, A.D. Paulsen, A.D. Javadekar, D.G. Vlachos, P.J. Dauenhauer, Energy Environ. Sci. 5 (2012) 5414.
[27] M.J. Antal Jr., W.S.L. Mok, G.N. Richards, Carbohydr. Res. 199 (1990) 91.
[28] M.J. Antal Jr., T. Leesomboon, W.S. Mok, G.N. Richards, Carbohydr. Res. 217 (1991) 71.
[29] J. Scheirs, G. Camino, W. Tumiatti, Eur. Polym. J. 37 (2001) 933.
[30] J. Barbier, N. Charon, N. Dupassieux, A. Loppinet-Serani, L. Mahé, J. Ponthus, M. Courtiade, A. Ducrozet, A.-A. Quoineaud, F. Cansell, Biomass Bioenergy 46 (2012) 479.
[31] P.F. Britt, A.C. Buchanan, M.J. Cooney, D.R. Martineau, J. Org. Chem. 65 (2000) 1376.
[32] S. Kang, X. Li, J. Fan, J. Chang, Renew. Sustain. Energy Rev. 27 (2013) 546.
[33] G.C.A. Luijkx, F. van Rantwijk, H. van Bekkum, Carbohydr. Res. 242 (1993) 131.
[34] I. Pastorova, R.E. Botto, P.W. Arisz, J.J. Boon, Carbohydr. Res. 262 (1994) 27.
[35] Y.-T. Cheng, G.W. Huber, Green Chem. 14 (2012) 3114.
[36] M. Sasaki, Z. Fang, Y. Fukushima, T. Adschiri, K. Arai, Ind. Eng. Chem. Res. 39 (2000) 2883.
[37] T.H. Pedersen, L.A. Rosendahl, Biomass Bioenergy 83 (2015) 206.
[38] S.K.R. Patil, C.R.F. Lund, Energy Fuels 25 (2011) 4745.
[39] S.K.R. Patil, J. Heltzel, C.R.F. Lund, Energy Fuels 26 (2012) 5281.
[40] T.M.C. Hoang, E.R.H. van Eck, W.P. Bula, J.G.E. Gardeniers, L. Lefferts, K. Seshan, Green Chem. 17 (2015) 959.
[41] M. Sevilla, A.B. Fuertes, Carbon 47 (2009) 2281.
[42] M. Sevilla, A.B. Fuertes, Chem. Eur. J. 15 (2009) 4195.
[43] S. Kersten, M. Garcia-Perez, Curr. Opin. Biotechnol. 24 (2013) 414.
[44] S. Zhou, B. Pecha, M. van Kuppevelt, A.G. McDonald, M. Garcia-Perez, Biomass Bioenergy 66 (2014) 398.
[45] J. Akhtar, N.A.S. Amin, Renew. Sustain. Energy Rev. 15 (2011) 1615.
[46] Z. Wang, B. Pecha, R.J.M. Westerhof, S.R.A. Kersten, C.-Z. Li, A.G. McDonald, M. Garcia-Perez, Ind. Eng. Chem. Res. 53 (2014) 2940.
[47] J. Piskorz, D.S.A.G. Radlein, D.S. Scott, S. Czernik, J. Anal. Appl. Pyrolysis 16 (1989) 127.
[48] D.S. Scott, J. Piskorz, M.A. Bergougnou, R. Graham, R.P. Overend, Ind. Eng. Chem. Res. 27 (1988) 8.